ChemPubSoc Europe

DOI: 10.1002/chem.201400153

CHEMISTRY A European Journal Full Paper

Fullerenes

Hierarchically Ordered Self-Assembly of Amphiphilic Bifullerenes

Lennard Wasserthal,[a] Boris Schade,[b] Kai Ludwig,[b] Christoph Böttcher,*[b] and Andreas Hirsch*[a]

Abstract: A series of novel functionalised dumbbell-shaped bifullerenes in which two [5.0] pentakis-adducts of C_{60} are covalently connected by cyclic bismalonates were synthesised. These dimeric compounds, carrying various combinations of hydrophilic and hydrophobic addends, self-assemble in aqueous solution towards supramolecular architectures of different structural complexity as observed by cryogenic transmission electron microscopy (cryo-TEM). The detailed analysis of the image data revealed an unprecedented hierarchical aggregation behaviour. Whereas completely hydrophilic substituted bifullerenes formed profoundly monodisperse populations of small oligomeric elementary micelles consisting of only three or four bifullerene molecules in a supposedly bent conformation, their amphiphilic equivalents underwent a hierarchical two-step assembly process towards larger spherical and even rod-like structures. The data suggest that the hierarchical assembly process is driven by hydrophobic interactions of preformed tetrameric elementary micelles.

Introduction

The spontaneous self-organisation of amphiphilic biomolecules, such as lipids, proteins or nucleic acids, into hierarchically ordered superstructures in water forms the basis for the development of life on Earth. This assembly process is driven by entropy governed hydrophobic interactions.[1] We have recently reported on a series of related supramolecular aggregation processes with the first examples of shape-persistent micelles that are based on new amphiphilic calixarene or fullerene frameworks.[2,3] The extraordinary structural precision of these objects, which is based on the specific shape, chemical polyfunctionality and rigidity of the constituting building blocks, allowed for the first time the determination of the three-dimensional organisation of their supramolecular assemblies with molecular resolution from cryo-TEM data. It was shown that shape-persistent micelles can have comparatively large pores, which, however, are impenetrable for water molecules. Nevertheless, the architecture of these micellar structures follows the typical bilayered arrangement of small molecular amphiphiles, namely the hydrophilic part pointing toward the water subphase and the hydrophobic parts being located in the water-free core volume of such nano-objects.

Fullerenes are ideal candidates serving as rigid scaffolds for the construction of novel supramolecular assembly structures. Nevertheless, to date only few examples of defined supramolecular assemblies of fullerenes have been described[3,4] owing to their poor solubility in common solvents. In this study we report for the first time on the non-classical aggregation behaviour of a series of new dumbbell-shaped bifullerene derivatives in water. Systematic TEM investigations disclose a hierarchical aggregation phenomenon for the amphiphilic compounds where the above-mentioned fundamental construction principle is not strictly valid anymore. Herein, all the bifullerenes may form unconventional elementary building blocks, which in some cases tend to form a higher level of supramolecular architecture. This observation not only provides new and detailed insight into the assembly behaviour of more complex amphiphilic building blocks but also indicates a novel intriguing strategic direction for the construction of complex and structurally defined supramolecular assemblies.

Results

The general synthesis of the new compounds was accomplished by connecting the corresponding [5.0] pentakis-adducts of C_{60}[5] to a cyclic bismalonate,[6] which has two free binding sites available for the targeted cyclopropanation of the remaining octahedral [6,6] double bonds of the fullerenes (Figure 1). In the case of symmetric bifullerenes, such as **1** or **2**,

[a] *L. Wasserthal, Prof. A. Hirsch*
Department of Chemistry and Pharmacy and Interdisciplinary Center for Molecular Materials (ICMM)
Friedrich-Alexander-Universität Erlangen-Nürnberg
Henkestr. 42, 91054 Erlangen (Germany)
E-mail: andreas.hirsch@chemie.uni-erlangen.de

[b] *Dr. B. Schade, Dr. K. Ludwig, Dr. C. Böttcher*
Forschungszentrum für Elektronenmikroskopie
Institut für Chemie und Biochemie, Freie Universität Berlin
Fabeckstr. 36a, 14195 Berlin (Germany)
E-mail: christoph.boettcher@fzem.fu-berlin.de

Supporting information for this article is available on the WWW under http://dx.doi.org/10.1002/chem.201400153.

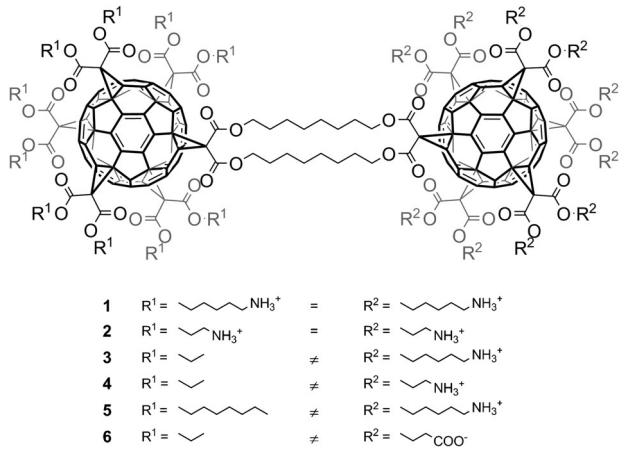

Figure 1. Chemical formulas of the synthesised new family of symmetrically hydrophilic **1**–**2** and amphiphilic ("amphi-bifullerenes") **3**–**6** substituted dumbbell-shaped bifullerenes.

both pentakis-precursors can be attached simultaneously. Otherwise, the bismalonate was applied in large excess allowing for the efficient formation of monofullerenes, which in a subsequent step were coupled to the second fullerene pentakis-adduct precursor. In an alternative approach parent C_{60} was coupled first and subsequently transferred into the hexakis-adduct with five terminating malonate addends in a divergent reaction.[7] The final acidic deprotection of the Boc or *t*Bu groups was accomplished by treatment with TFA. Detailed reaction procedures for all compounds are given in the Supporting Information.

All ammonium salt derivatives (**1**–**5**) easily dissolve in pure water to form clear solutions, concomitantly generating an acidic pH. The amphiphilic carboxylate compound **6** dissolves only in buffered solution adjusted to a basic pH (~8.0). The aggregation of compounds **1** and **3**–**5**, respectively, was monitored by determination of the critical micelle concentration and, for all compounds, by performing cryo-TEM measurements, which allowed a direct visualisation of corresponding supramolecular assemblies in the native environment of the solvent (Table 1).[8–10] The assemblies of all compounds provided an unusually high contrast in the micrographs allowing for an unprecedented direct view of differentiated structural details in individual entities (Figure 2 and Figure S1 in the Supporting Information).

Symmetrically hydrophilic substituted bifullerenes **1** and **2** formed monodisperse populations of discrete small particles with an average diameter of 3–4 nm (Figure 2a and Figure S1a in the Supporting Information). The particle density is homogeneous, that is, an internal structural differentiation is not detectable. Amphiphilic substituted bifullerenes ("amphi-bifuller-

Table 1. Critical micelle concentrations (cmc) of amphi-bifullerenes **1**, and **3**–**5** in water.

	1	**3**	**4**	**5**
CMC [μmol L^{-1}]	50.6	4.0	10.0	0.7

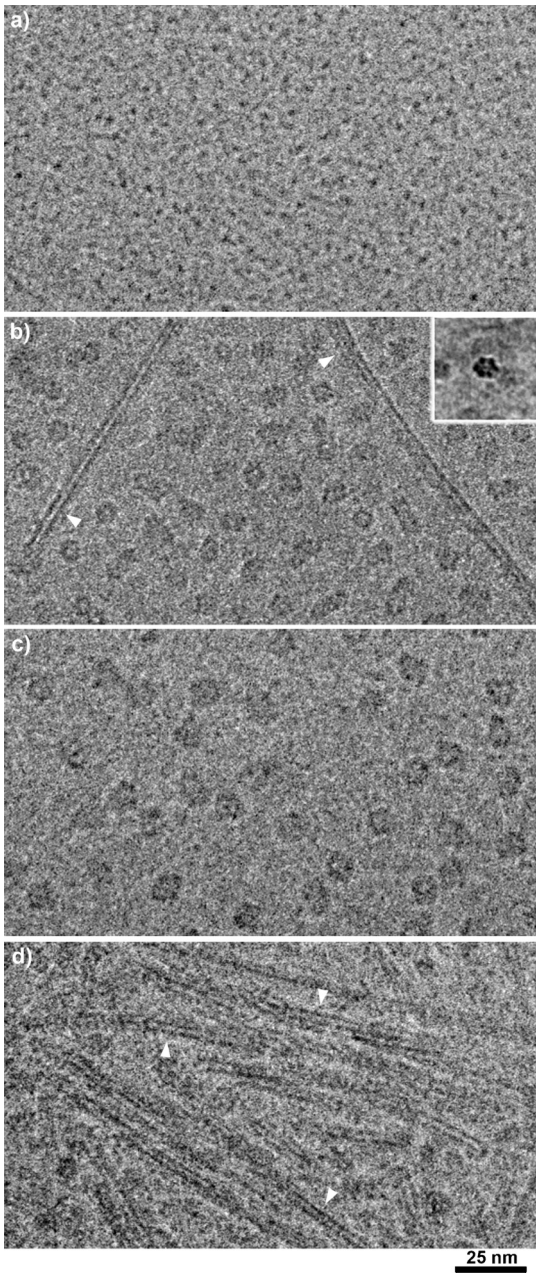

Figure 2. Cryo-electron micrographs of aqueous solutions of: a) **1**, b) **4**, c) **5**, and d) **6**. a) Symmetrically substituted hydrophilic bifullerenes **1** (and also **2**, see Figure S1a in the Supporting Information) form small granular particles with average diameters of 3–4 nm. b) Amphiphilic substituted bifullerenes bearing short hydrophobic *n*-propyl groups (**3**, **4**, and **6**) form globular aggregates of comparable diameters ranging from 5 nm up to 9 nm. Besides globular aggregates, amphi-bifullerene **4** forms elongated aggregates often presenting a double or triple striated profile (white arrowheads) with a stripe thickness of 2–3 nm. Occasionally, hexagonal motifs of high contrast (inset) are detected within thicker ice-films, which originate from rod-like assemblies orientated parallel to the electron beam thus presenting their cross-sectional views. c) A significantly larger assembly diameter (10 to 13 nm) was observed with the longer *n*-octyl substituted compound **5**. d) Carboxyl groups carrying **6** forms mostly elongated aggregates. These aggregates have the same diameters and exhibit the same longitudinal striations (white arrowheads) like the ones described for bifullerene **4**. Titration of the solutions to acidic (**3** and **4**) or basic (**6**) pH values leads to a slightly increased agglomeration of the particles without changing the individual assembly structures (Figure S2 in the Supporting Information).

enes") **3**–**6**, however, gave significantly larger, nearly spherical assemblies. In this case the majority of assemblies are differentiated into an electron dense corona with different shapes and variable structural complexity and an unstructured central core of lower density. The three compounds bearing short hydrophobic propyl groups (**3**, **4** and **6**) produced particles in a narrow diameter range of 5 nm up to 9 nm (for details see below). A significant increase in the assembly diameter (10 to 13 nm), however, was observed in the case of **5** in which the hydrophobic side chains are considerably longer (Figure 2c).

Differentiated structural patterns are directly visible in the raw images of individual spherical particles of the amphiphilic compounds **3**–**5**. They point to a preferential ultrastructural organisation of the aggregates and initiated a further treatment by a statistical method (multivariate statistical analysis, MSA),[11,12] which determines the structural differences of an image data set (considering several thousand individual particles) in terms of size, shape or inherent symmetry elements (details are given in the Supporting Information). The analysis allows for the identification (classification) of structurally identical particles, which are eventually aligned and summed up (Figure 3). In this way structural features are enhanced whereas statistical noise is averaged out, in other words (class sum) images with an improved signal-to-noise ratio are obtained. Diverse periodical motifs were obtained representing different spatial orientations of preferential assembly structures. Very striking are the two populations of globular particles observed with **3** having mean diameters of 7.6(±0.9) nm (Figure 3a) and 9.2(±0.5) nm (Figure 3b), respectively, which also differ in their structural complexity. Some larger agglomerates are also detectable (Figure 3c).

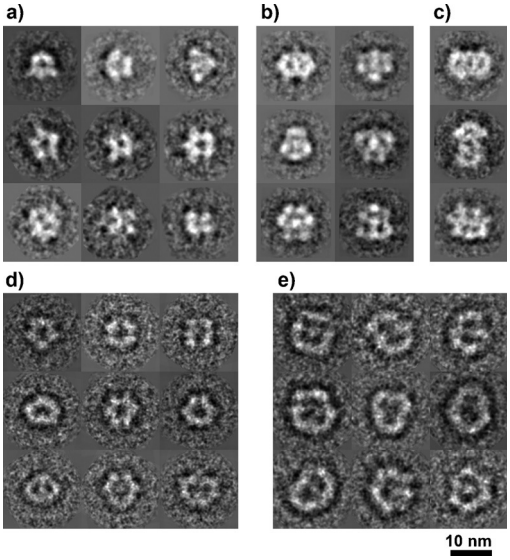

Figure 3. Galleries of selected class-sum images (details of the averaging procedure are given in the Supporting Information) disclose internal structural patterns of spherical particles obtained from: a)–c) **3**, d) **4**, and e) **5**. For compound **3** class-sum images (a–c) of smaller (a), and larger aggregates (b) as well as higher-order structures (c) were detected. Particles of **5** (e) appear to be significantly larger compared to **3** and **4**.

In contrast to compound **3** aggregate sizes of **4** and **5** did not disperse. Indeed, amphi-bifullerene **4** formed spherical assemblies in a narrow size range of 8.7(±1.2) nm (Figure 3d), whereas assemblies of **5** turned out to be significantly larger with a mean diameter of the order of 12.0(±1.2) nm (Figure 3e). The thickness of the corona is similar in the cases of **3** and **4** measuring 2.2(±0.2) nm, but is significantly larger in the case of **5** (2.8(±0.3) nm).

In addition to spherical assemblies, amphi-bifullerenes with short hydrophilic side chains (**4** and **6**) form elongated aggregates, which are remarkably rigid and often present double or triple striated density profiles with a stripe thickness of 2–3 nm (marked by arrows in Figure 2b and d). The elongated aggregates appear frequently in samples of **4** and are even predominant with the carboxylated compound **6** (also compare Figure S3 in the Supporting Information). Their overall length varies from only ten nanometres up to micrometres and the diameters range from 5 nm up to 7 nm. It is worth noting that for an unambiguous interpretation of the elongated aggregates observed with amphi-bifullerenes **4** and **6** in some cases the two- and threefold longitudinal striation patterns blend into each other if one follows the assemblies' long-axis. This detail indicates that the different patterns obviously represent various spatial orientations of structurally identical assemblies, if rotated around their long axis (Figure S12 in the Supporting Information). Occasionally, hexagonally structured motifs with striking high contrast are observed (Figure 2b, inset). From the extraordinary strong contrast and the preferential appearance in thick ice films we deduce that such patterns represent cross sectional views (top views) of elongated aggregates that are orientated parallel to the incident electron beam. This finding provides a very useful supplement for the interpretation of their three-dimensional structural organisation (see below). Regardless of the molecular differences between **4** and **6** (ammonium vs. carboxylate groups) their aggregates' structural motifs and dimensions turned out to be very similar (Figure 4).

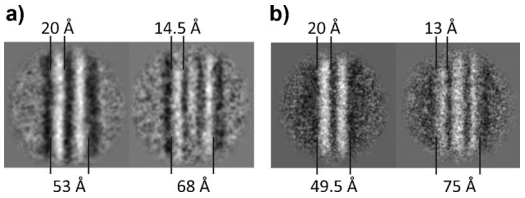

Figure 4. Class-sum images obtained from segments of elongated assemblies formed by: a) the cationic compound **4**, and b) the anionic compound **6**, revealing accurate dimensions of the two- and threefold striation motifs exemplarily presented in Figure 2c and d. Although different in the molecular composition the packing geometries and dimensions display striking similarities for both compounds.

Discussion

The first important conclusion to be deduced from the size of the core-shell structured amphi-bifullerene assemblies is that they obviously exceed the dimensions of conventional spherical micelles with a molecular bilayer constitution (4–5 nm) usu-

ally observed with amphiphilic surfactants, such as sodium dodecyl sulfate. Similarly, in the case of the elongated aggregates (compounds **4** and **6**), the dimensions and patterns observed with the longitudinal segmentation do not correspond to a simple bilayered fibre density profile.[9]

It is inevitable to conclude from geometrical considerations and from the fact that fullerene cages contribute the major contrast in the electron micrographs that the observed patterns of the spherical particles could only be accomplished by arrangements in which all fullerene cages are located within the assemblies' high contrast corona. Such an arrangement can, for example, be achieved by a vesicular organisation in which a fullerene loaded corona entraps an aqueous core volume. Assuming that the bifullerenes adopt a more or less stretched conformation and form a typical bilayered vesicle membrane, however, does not satisfactorily coincide with the observed structural characteristics in terms of membrane thickness or density profile (for a more detailed discussion of alternative packing motifs see also the Supporting Information).

In fact, all considerations coalesce in the formulation of a novel molecular architecture due to a hierarchical assembly process. Apart from the mentioned geometrical aspects particular hints for this finding came from the observation that the symmetrical hydrophilic substituted derivatives **1** and **2** exclusively form granular and structurally undifferentiated aggregates with diameters of only 3–4 nm (Figure 2a). Though the particles are small they are, however, too large to originate from individual molecules, thus indicating the formation of oligomeric assemblies consisting of three to four molecules (Figure 5). Here, we assume that the special architecture of two fullerenes connected by a flexible spacer facilitates the formation of a bent conformation initialised by intramolecular aliphatic interactions (Figure 5a). This conformation promotes intermolecular hydrophobic interactions by the intramolecular change from a bola-amphiphilic towards a more amphiphilic character; this process initiates the exposing of intramolecular hydrophobic surfaces (Figure 5b).[13,14] Thereby, the length of the spacer should play a critical role, being large enough to sufficiently promote the mentioned amphiphilic character and also facilitate proper orientation of the fullerenes. By aggregation the hydrophobic core can be shielded from the aqueous phase while the hydrophilic groups are smoothly exposed towards the outer aggregate surface (Figure 5c). The geometrical implications (size and shape) and the packing requirements of the globular fullerene cores (which have to expose their hydrophilic moieties towards the particles surface) limit the number of the possible architectures to tri- or tetrameric oligomers. Thus, 60 (trimer) or 80 (tetramer) ammonium groups of the hydrophilic bifullerenes would spread evenly over the entire assembly surface forming and stabilising a uniform hydration shell (Figure 5e). The size and shape of such elementary micelles observed with compounds **1** and **2** correlates quite well with the dimensions of respective modelled particles (see the Supporting Information).

We deduce from detailed structural evaluations that amphi-bifullerenes **3**–**6** associate in a similar way to form elementary micelles as found for compounds **1** and **2**. A tetrameric geometry of the amphi-bifullerenes (Figure 5f and g) constitutes a smooth distribution of hydrophilic groups around the hydrophobic core as well. Nevertheless, overall hydrophilic shielding should be less pronounced in case of amphi-bifullerenes if

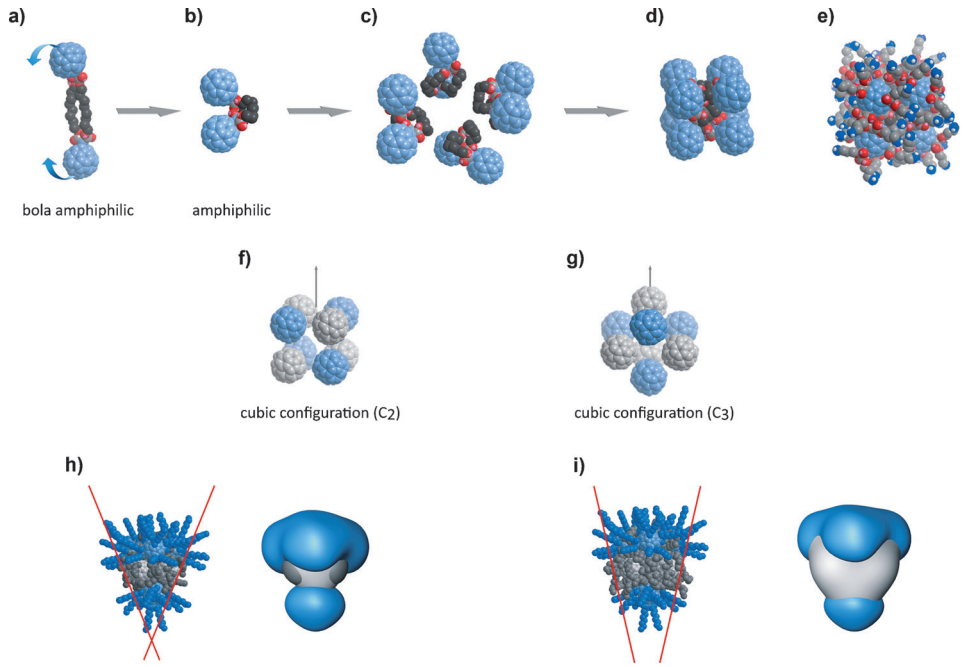

Figure 5. Schematic aggregation principles of bifullerenes in water. a), b) CPK modelling of a skeletal bifullerene (without side chains) indicating the bending phenomenon. c), d) Four bent bifullerenes assemble by hydrophobic interactions and bury their alkyl-bridges in the core volume of a tetrameric elementary assembly. (An alternative though less likely trimeric assembly is shown in Figure S7 in the Supporting Information.) e) From the complete model of the elementary micelle of compound **1** with its short side chains the smooth distribution of the 80 hydrophilic ammonia groups at the micelle's surface becomes evident. Also, asymmetric amphi-bifullerenes **3**–**6** can associate to form elementary micelles. f) In contrast to a trimeric arrangement (Figure S7 in the Supporting Information), the cubic alignment of the tetrameric micelle allows for evenly distributing ammonium groups around the micelle (C_2-symmetry axis indicated by arrow). g). If the cube is viewed with its C_3-symmetry axis (arrow) in upright orientation (one hydrophilic fullerene pointing downward and three upward) the fullerene scaffold reveals a conical shape. As shown for compounds **3** (h) and **5** (i), the length of the hydrophobic side chains affects the conical tilt angle (illustrated by the red lines) and the size of the hydrophobic surface (grey facing in the schematic representations of the respective CPK models placed on the right) and therefore eventually determines the curvature of the globular particles in the subsequent aggregation step.

compared to symmetrically substituted compounds **1** and **2**, due to the halved number of ammonium groups. This disadvantage becomes even more pronounced, if the hydrophilic addends are short as in compounds **4** and **6**. Accordingly, in a consequential step elementary amphi-bifullerene micelles should arrange into structures of higher order to antagonise the exposure of hydrophobic domains towards the polar environment. Such a sequential hierarchical aggregation includes the formation of spherical as well as rod-like assemblies (see below). Thereby, the observed differences in the structural organisation may arise from geometrical peculiarities of the elementary micelles as will be discussed in the following.

Viewing the cubic elementary micelle orthogonally to its C_3-symmetry axis (Figure 5g) reveals its cone shaped geometry, the tilt angle of which might determine the curvature as well as the number of elementary micelles constituting the higher order spherical assemblies. Hereby, shorter hydrophobic side chains increase this tilt angle (Figure 5h) eventually leading to the formation of smaller globular aggregates. In assemblies of compound **5** with longer hydrophobic side chains the micelles' tilt angle is attenuated (Figure 5i), thus generating assemblies with reduced curvature (compare **3** or **4** vs. **5**). Note, that the thickness of the corona in the assemblies of compound **5** is also increased, which can be explained by longer hydrophobic chains causing larger elementary micelles. Shorter hydrophilic side chains in **4**, on the other hand, also enlarge the hydrophobic surface due to a less efficient shielding by hydrophilic groups driving the assembly process not only towards spherical but also towards elongated aggregates.

Modelling different arrangements of elementary micelles on the basis of the before-mentioned geometrical restrictions and comparing the corresponding calculated projection patterns with the microscopic data (see the Supporting Information for details) turned out to be a reasonable method to support the above-outlined observations and to reinforce the principles of preferential molecular arrangements. A completely intuitive strategy of iteratively modifying molecular alignments eventually resulted in a very good agreement between models and experimental data. One has, however, to be fully aware, that such models are solely a description of structural preferences in the assembly process. Deviations from the proposed models are unquestionably existent and are found in the data set as demonstrated, for example, in Figure 3c. However, the finding that statistical evaluations of thousands of individual particles delivers sets of structurally defined patterns (this means that identical assembly structures have to be present in the data sets), justifies the search for preferential collocations. In this way we can propose that compound **3** forms higher-order assemblies consisting, to a preferable extent, of twelve or twenty elementary micelles, whereas **4** and **5** rather form homogenous populations of spherical assemblies consisting of twenty elementary micelles. Differences in the assembly size between **4** and **5**, therefore, arise from differences in the size and geometry of the preformed elementary micelles initialised by differences in the molecular structures (different chain lengths). In the eventually obtained spherical assemblies elementary micelles form a structured corona, which exposes their hydrophilic surface towards the inner water-filled core volume and towards the outer aqueous bulk phase.

The structural data of rod-like assemblies, however, can be best interpreted by assuming a tube-like arrangement of six hexagonally arranged threads each composed by linear stacks of very much the same elementary micelles proposed for the spherical assemblies above (Figure S10 in the Supporting Information). The high contrast hexagonally shaped top views (Figure 2b, inset) support the above assumption. Essentially, such an arrangement produces exactly those two distinguishable namely twofold and threefold striated projections if rotated around the longitudinal axis (Figure S11 in the Supporting Information).

As has been stated above hydrophilic shielding may be most insufficient with the short hydrophilic (**4** and **6**) propyl chains. Linear growth of elementary micelles effectively diminishes the surface area per volume[15] and threads are therefore likely to be preferable for these compounds (Figure S12 in the Supporting Information). For **6** this preference may be additionally accompanied by linear hydrogen bonding of the carboxyl groups forcing the almost exclusive formation of rods. The crystal-like stacking from densely packed fullerenes also explains the stiffness of the elongated aggregates. Moreover, construction of the threads in this way, would exactly match the arrangement of fullerenes proposed earlier by Prato et al.[16] Model data again coincide with this assumption (Figure S11 in the Supporting Information).

Conclusion

Dumbbell-shaped amphi-bifullerenes assemble in aqueous solution to form spherical or rod-like aggregates with recurring structural motifs. The expectation that amphi-bifullerenes would adopt a classical micellar architecture is quite obviously not met. Instead, the structural data analysis reveals that preformed oligomeric elementary building blocks assemble in a hierarchical manner toward larger and structurally more complex assemblies. First evidence comes from the behaviour of the completely hydrophilic substituted bifullerene derivatives, which exclusively form very small particles of 3–4 nm in diameter. Such elementary structures are obviously characteristic for all presented bifullerenes. They are stable and monodisperse in the case of completely hydrophilic substituted bifullerenes, but continue to aggregate towards higher architectures in the case of the amphiphilic substituted bifullerenes. This second aggregation step is obviously dictated by the exposure of hydrophobic surfaces, which is inevitable in the first assembly step of amphiphilic compounds due to the reduced number of hydrophilic substituents.

The proposed hierarchical construction from tetrameric micelles not only explains the course of the curvature (size) of the different globular aggregates and the high contrast in the images, but also illustrates the anisotropic density distribution within the shell that emerges from the elementary micelles' packing motifs. The geometry of the superaggregates is driven by the length of the hydrophobic side chains (not to be confused with the hydrophobic bridge sequences), which deter-

mine the size of the exposed hydrophobic domains and by the packing restrictions caused by the conical tilt angle of the elementary micelles. Although the microscopy data reveal structural preferences, there are minor but discriminable alternative arrangements of the elementary micelles possible (linear vs. spherical assemblies, smaller vs. larger assemblies), which can be explained by the largely non-directional interactions of the elementary micelles' hydrophobic domains. Our approach of comparing experimental and model projection data offers the clues for the spatial molecular arrangements in such assemblies. This is, to our knowledge, the first report on an amphiphilic system, which forms supramolecular structures by undergoing a consecutive assembly process (i.e., hierarchical two-step mechanism) via the formation of an energetically unfavourable intermediate aggregate.

Experimental Section

Conductometric titration

Conductometric titrations were performed by diluting a sample to such an extent that it was 10.5-times more concentrated than the highest desired end concentration. The measurement cell was filled with water (9.5 mL). Then, the concentrated solution was added in 20 μL portions. The kink in the titration curves is associated with the critical micellar concentration (cmc). Values are given in Table 1.

Cryogenic transmission electron microscopy

Samples for cryo-TEM investigations were prepared according to our standard method (see the Supporting Information). Microscopy was conducted using a FEI Tecnai F20 at a primary magnification of 100 000× (160 kV, FEG-illumination) equipped with a FEI Eagle 2k CCD camera (pixel resolution 2.268 Å) or a Philips CM12 (100 kV, LaB6-illumination) at a primary magnification of 58 300×. CM12 data were recorded on Kodak® electron image film SO 163 (Eastman Kodak Company, USA) and digitised for image processing to a final pixel resolution of 0.686 Å per pixel.

Data processing and image analysis

Single particles were collected from the digital data (see above) using the boxer module from the EMAN software package.[17] Data processing, namely alignment steps, image averaging, multivariate statistical analysis, classification etc., was performed in the context of the IMAGIC 5 software package (Image Science GmbH, Berlin, Germany).[18]

Molecular model design

Modelling procedures were performed with Chem3D Pro 12.0 from the ChemBioOffice 2010 suite (PerkinElmer Informatics, Massachusetts, USA). Resulting PDB files were Gaussian filtered at a resolution of 21 Å employing the pdb2vol module from the SITUS program package.[19] Finally, 2D projection images were calculated (using the IMAGIC-5 software package) 18 to create projection images of the 3D models.

Acknowledgements

This work was generously supported by grants of the Deutsche Forschungsgemeinschaft (DFG) to C.B. (BO 1000/9-3) and A.H. (HI 468/13-4), which is gratefully acknowledged by the authors.

Keywords: aggregation · cryo-transmission electron microscopy · fullerenes · image processing · nanostructures

[1] G. Némethy, *Angew. Chem.* **1967**, *79*, 260 – 271; *Angew. Chem. Int. Ed. Engl.* **1967**, *6*, 195 – 206.
[2] a) M. Kellermann, W. Bauer, A. Hirsch, B. Schade, K. Ludwig, C. Böttcher, *Angew. Chem.* **2004**, *116*, 3019 – 3022; *Angew. Chem. Int. Ed.* **2004**, *43*, 2959 – 2962; b) B. Schade, K. Ludwig, C. Böttcher, U. Hartnagel, A. Hirsch, *Angew. Chem.* **2007**, *119*, 4472 – 4475; *Angew. Chem. Int. Ed.* **2007**, *46*, 4393 – 4396.
[3] S. Burghardt, A. Hirsch, B. Schade, K. Ludwig, C. Böttcher, *Angew. Chem.* **2005**, *117*, 3036 – 3039; *Angew. Chem. Int. Ed.* **2005**, *44*, 2976 – 2979.
[4] a) H. Li, J. Choi, T. Nakanishi, *Langmuir* **2013**, *29*, 5394 – 5406; b) J. Li, B. C. Benicewicz, *J. Polym. Sci. A* **2013**, *51*, 3572 – 3582; c) A. Muñoz, B. M. Illescas, M. Sánchez-Navarro, J. Rojo, N. Martín, *J. Am. Chem. Soc.* **2011**, *133*, 16758 – 16761; d) T. Homma, K. Harano, H. Isobe, E. Nakamura, *J Am Chem. Soc.* **2011**, *133*, 6364 – 6370; e) M. Brettreich, S. Burghardt, C. Böttcher, T. Bayerl, S. Bayerl, A. Hirsch, *Angew. Chem.* **2000**, *112*, 1915 – 1918; *Angew. Chem. Int. Ed.* **2000**, *39*, 1845 – 1848; f) M. Hetzer, S. Bayerl, X. Camps, O. Vostrowsky, A. Hirsch, T. M. Bayerl, *Adv. Mater.* **1997**, *9*, 913 – 917.
[5] F. Hörmann, W. Donaubauer, F. Hampel, A. Hirsch, *Chem. Eur. J.* **2012**, *18*, 3329 – 3337.
[6] U. Reuther, T. Brandmüller, W. Donaubauer, F. Hampel, A. Hirsch, *Chem. Eur. J.* **2002**, *8*, 2261 – 2273.
[7] I. Lamparth, C. Maichle-Mössmer, A. Hirsch, *Angew. Chem.* **1995**, *107*, 1755 – 1757; *Angew. Chem. Int. Ed. Engl.* **1995**, *34*, 1607 – 1609.
[8] J. Dubochet, A. W. McDowall, *J. Microsc.* **1981**, *124*, 3 – 4.
[9] D. Danino, *Curr. Opin. Colloid Interface Sci.* **2012**, *17*, 316 – 329.
[10] J. R. Bellare, H. T. Davis, L. E. Scriven, Y. Talmon, *J. Electron Micr. Tech.* **1988**, *10*, 87 – 111.
[11] M. van Heel, J. Frank, *Ultramicroscopy* **1981**, *6*, 187 – 194.
[12] M. van Heel, B. Gowen, R. Matadeen, E. V. Orlova, R. Finn, T. Pape, D. Cohen, H. Stark, R. Schmidt, M. Schatz, A. Patwardhan, *Q. Rev. Biophys.* **2000**, *33*, 307 – 369.
[13] F. Stillinger, *J. Solution Chem.* **1973**, *2*, 141 – 158.
[14] K. Lum, D. Chandler, J. D. Weeks, *J. Phys. Chem. B* **1999**, *103*, 4570 – 4577.
[15] C. Tanford, *J. Phys. Chem.* **1972**, *76*, 3020 – 3024.
[16] V. Georgakilas, F. Pellarini, M. Prato, D. M. Guldi, M. Melle-Franco, F. Zerbetto, *Proc. Natl. Acad. Sci. USA* **2002**, *99*, 5075 – 5080.
[17] S. J. Ludtke, P. R. Baldwin, W. Chiu, *J. Struct. Biol.* **1999**, *128*, 82 – 97.
[18] M. van Heel, G. Harauz, E. V. Orlova, R. Schmidt, M. Schatz, *J. Struct. Biol.* **1996**, *116*, 17 – 24.
[19] W. Wriggers, *Acta Crystallogr. Sect. D* **2012**, *68*, 344 – 351.

Received: January 14, 2014

